doi:10.3772/j.issn.1006-6748.2019.01.015

Fractal-Creep wears model and accuracy degradation simulation of linear ball guide①

Zhang Wei(张 巍)②*** , Wang Min* , Jiang Xiongfei*
(* Key Laboratory of Advanced Manufacturing Technology of Beijing Municipality College of Mechanical Engineering and Applied Electronics Technology, Beijing University of Technology, Beijing 100124, P. R. China)
(** Engineering & Training Center, Inner Mongolia University of Science and Technology, Baotou 014010, P. R. China)

Abstract

Based on Hertz contact theory, contact area parameters between ball and raceway are calculated. Using the Creep theory of Cater and V-J theory, adhesive area and micro-slip area in the contact area are analyzed. It is considered that micro-adhesion wear of micro convex body in the slip area is the main reason for accuracy degradation of a linear ball guide pair. And, the characteristics of the contact area between ball and raceway of slider are characterized using the fractal function. Fractal parameters are obtained using the least squares fitting double logarithmic graph structure function. Considering the lubrication condition between the ball and rail of slider, stress analysis is carried out on the adhesive area. A fractal-creep model of contact surfaces is established in the micro-slip region. The fractal parameters of a certain guide rail are measured, and the wear degradation process of linear rolling guide is simulated. Finally, the relationship between wear and relative tangential velocity, normal load and running mileage of linear ball guide is obtained.

Key words: linear rolling guide, Creep theory, Hertz contact, fractal characterization, accuracy degradation

0 Introduction

Accuracy retention of linear rolling guide pairs (LRGP) depends on the accuracy degradation and contact stiffness due to wear during working. At present, research of LRGP is focused mainly on stiffness and traditional friction problems. Few researches have been done on the micro-friction of LRGP. Few people have combined the Creep theory with the fractal theory, and used it to analyze the micro-friction degradation of LRGP. Based on Hertz theory and the rigid body dynamics, combined with the Archard theory and the prediction model, Zhong[1] established the stiffness model of linear guide, but the Archard friction formula is mainly applicable to sliding friction, which is not suitable for rolling friction.

Since Mandelbrot proposed fractal geometry theory, the fractal geometry theory has been widely used in different subjects. Fractal theory was introduced into the contact mechanics and tribology[2]. Zhou et al.[3] set up a predictive model of friction based on M-B fractal model. The fractal geometry theory can effectively characterize the surface of the machine, and the model based on the fractal geometry theory is more reasonable and effective than traditional models[4]. Fang et al.[5] established a mechanical seal surface adhesive wear fractal model according to the mechanical fractal model and Archard theory. In LRGP, the contact points are not the only one point but an ellipse area. During ball rolling, relative sliding occurs between ball and rail. Many studies suggest that, ellipse areas can be divided into adhesive area and sliding area and the two areas affect the division and distribution of wear and abrasion.

Creep theory further analyzes the movement condition in the Hertz contact area. Due to the complexity of motion, the contact area is divided into adhesive region and micro sliding region; the actual contact area is not the Hertz contact area, but the micro sliding region. There are many factors affecting the area of the adhesive region in the contact area, such as the magnitude of the relative tangential force, the coefficient of fric-

① Supported by the National Natural Science Foundation of China (No. 51505012, 51575014), the Natural Science Foundation of Beijing (No. 3154029, KZ201410005010), the Important National Science & Technology Specific Projects of China (No. 2012ZX04010021-001-004) and Beijing Postdoctoral Research Foundation (No. 2015XX-13).
② To whom correspondence should be addressed. E-mail: zhangwei2009035@163.com
Received on Jan. 22, 2018

tion on the joint surface, and the magnitude of the outside load of the slider. When the ball bears force, it will produce a slight elastic deformation. The adhesion nodes formed on the surface due to adhesion effect will be cut or dropped, and then debris will be formed.

The introduction of Creep theory is presented in this paper and rolling sliding distance is calculated considering the relative tangential force. The influence of external load on friction coefficient and the effect of Creep rate on adhesion area are also considered. Creep parameters are combined with the fractal parameters of raceway. In a small rotation condition, friction law is considered. Considering the lubrication state, the wear degradation laws of the LRGP are investigated.

1 Creep contact model

1.1 Simplification of contact ellipse with Cater theory

Coordinate system O_0 in the center of the Hertz contact area is established. Axis X is parallel to the movement direction, axis Y is horizontal direction and axis Z is through the origin of coordinates and vertically pointed to the paper face. According to the Cater F. W. theory, the ball-raceway oval contact area is reduced to a rectangular contact area, as shown in Fig. 1. Assuming, $L = 4b/3$, and the adhesion area width being $2a_\varepsilon$, the length is $2a$. Contact pressure distribution is given by Hertz contact $P(s)$. The maximum pressure is taken in the center of the contact area.

$$P(s) = P_0\left(1 - \frac{x}{\alpha^2} - \frac{y}{b^2}\right)^{0.5} \tag{1}$$

$$P_0 = \frac{3P(s)}{2\pi ab} \tag{2}$$

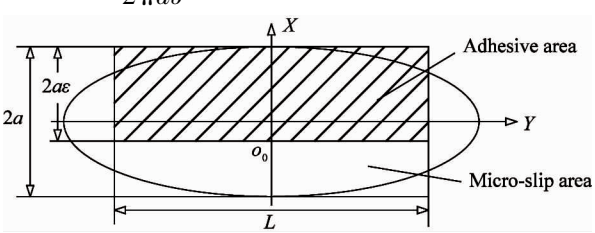

Fig. 1 Contact area and micro-slip area on raceway

According to the simplified conditions of the contact area and neglected influence lateral forces in the rectangular contact area, contact pressure can be simplified as

$$P(s) = \frac{2P}{\pi\alpha L}\left(1 - \frac{x^2}{\alpha^2}\right)^{1/2} \tag{3}$$

According to the Creep theory, the contact pressure distribution between ball and raceway is shown in Fig. 2.

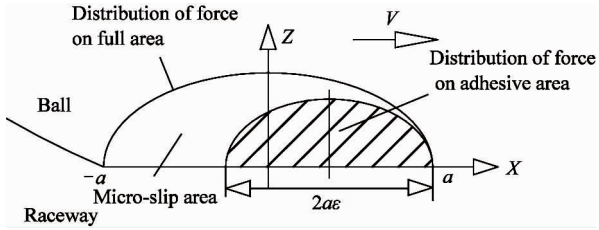

Fig. 2 Contact pressure distribution between ball and rail

When contact occurs between the ball and roller, it is assumed that the elastic deformation of ball at the point x is δ_b, and the elastic deformation of raceway at the contact point x is δ_s. According to Creep contact theory[6], normal deformation equation is

$$\delta_b - \delta_s = \delta - \frac{1}{2R}x^2 \tag{4}$$

where, R is relative curvature, R_b, R_g are the radiuses of curvature of the balls and raceway, respectively.

$$\frac{1}{R} = \frac{1}{R_g} + \frac{1}{R_b} \tag{5}$$

Seek partial derivative on both sides of Eq. (4), Eq. (6) can be obtained:

$$\frac{\partial\delta_b}{\partial x} - \frac{\partial\delta_s}{\partial x} = -\frac{1}{R}x \tag{6}$$

According to the elastic mechanics, it is known that Eq. (7) and (8) are accurately established, when $P(s)$ is perpendicular to the surface of the width of $2a$.

$$\frac{\partial\delta_b}{\partial x} = -\frac{2(1-\nu_1^2)}{\pi E_1}\int_{-a}^{a}\frac{P(s)}{x-s}\mathrm{d}s \tag{7}$$

$$\frac{\partial\delta_s}{\partial x} = -\frac{2(1-\nu_2^2)}{\pi E_2}\int_{-a}^{a}\frac{P'(s)}{x-s}\mathrm{d}s \tag{8}$$

where, v_1 and ν_2 are Poisson's ratio of ball and raceway, E_1 and E_2 are the elastic modulus of ball and slider's rail respectively. Through the analysis of Eq. (7) and (8), it is known that the size of the two stress is equal and in opposite direction. Substituting Eq. (7) and (8) into Eq. (6), Eq. (9) is got:

$$-\frac{2}{\pi E^*}\int_{-a}^{a}\frac{P(s)}{x-s}\mathrm{d}s = -\frac{1}{R}x \tag{9}$$

Substituting Eq. (3) into Eq. (9) gives the contact area of the half shaft α:

$$\alpha = \left(\frac{4RP}{\pi E^* L}\right)^{1/2} \tag{10}$$

In Eq. (10), E^* can be represented as

$$\frac{1}{E^*} = \frac{1-\nu_1^2}{E_1} + \frac{1-\nu_2^2}{E_2} \tag{11}$$

where, E_1 and E_2 are elastic modulus of ball and raceway, respectively.

1.2 Calculation of contact elliptical adhesion area and creep rate

According to Carter F. W. theory, the tangential force across the contact area at the creep stage should be the reduction of the tangential force of the sliding zone (full sliding state) to the adhesive area. The tangential force $P(x)$ of the contact area after the reducing adhesion area is

$$P_k(x) = -\frac{2\mu P_Z}{\pi a^2}(a^2 - x^2)^{1/2} + \frac{2\mu P_Z}{\pi a_\varepsilon^2}(a_\varepsilon^2 - (x - a + a_\varepsilon)^2)^{1/2} \quad (12)$$

The integral for Eq. (12) in the range of $[-a, a]$, Eq. (13) can be obtained:

$$\frac{a_\varepsilon}{a} = \left(1 - \frac{P_{Lx}}{\mu P_z}\right)^{1/2} \quad (13)$$

Similarly, the ratio of the elliptical short half-axis to the Hertz contact elliptical short half-axis can be obtained in the laterally adhered state:

$$\frac{b_\varepsilon}{b} = \left(1 - \frac{P_{Ly}}{\mu P_z}\right)^{1/2} \quad (14)$$

Assuming ζ_x is the creep rate of the ball along the rolling direction, the creep rate is defined as

$$\xi_x = 2(v_{gx} - v_{bx})/(v_{gx} + v_{bx}) \quad (15)$$

where, v_{bx} and v_{gx}, respectively, are the speed of ball at the rolling contact point in the rolling direction and the speed of raceway at contact point in the rolling direction. The creep rate ζ_x can be expressed as a gradient of tangential displacement difference between two points of contact[7]:

$$\zeta_x = 2\mu P_0(\alpha_\varepsilon - \alpha)/\alpha E^* \quad (16)$$

Substituting Eq. (10) and Eq. (13) into Eq. (16), Eq. (17) is got:

$$\zeta_x = \frac{2a\mu}{D_b}[(1 - (P_{Lx}/\mu P_Z))^{1/2} - 1] \quad (17)$$

Similarly, according Creep theory, the lateral creep rate ζ_y can be obtained:

$$\zeta_y = \frac{2b\mu}{D_b}[(1 - (P_{Ly}/\mu P_Z))^{1/2} - 1] \quad (18)$$

1.3 Calculation of pressure distribution in creep contact area

The maximal pressure and average pressure of the adhesive zone and the micro-slip zone can be obtained after obtaining the size distribution of the adhesion zone and the micro-slip area in the contact area. Assume that the shape of the adhesive region is also an oval. According to V-J theory, the elliptical adhesive region of the division[8] is

$$(b_\varepsilon/b)^{1/3} = (\alpha_\varepsilon/\alpha)^{1/3} \quad (19)$$

The pressure distribution $P_\varepsilon(x)$ can be obtained as

$$P_\varepsilon(x) = \begin{cases} \dfrac{2P_Z}{\pi\alpha^2}(\alpha^2 - x^2)^{1/2} & x \in S \\ \dfrac{2P_Z}{\pi\alpha^2}[(\alpha^2 - x^2)^{1/2} - (\alpha_\varepsilon^2 - x^2)^{1/2}] & x \in H \end{cases} \quad (20)$$

In Eq. (20), S represents the slippery region in the contact region, and H represents the adhesive region in the contact region.

According to the Hertz theory, if P_0 is the maximal contact pressure of the contact area, the Hertz contact ellipse will bear the maximum $P_0 = 3P/2ab$, the average pressure P_m is:

$$P_m = 2P_0/3 \quad (21)$$

Therefore, using Eq. (18) and Eq. (20), the average pressure $P_{m\varepsilon}$ of the micro-slip region is

$$P_{ms} = (1/(\pi a_\varepsilon b_\varepsilon) - 1/(\pi ab))P_z \quad (22)$$

2 Mechanical contact model

2.1 Hertz contact of the ball and the raceway

Coordinate system O in the center of the symmetry center of slider is established. Axis X is along the movement direction, axis Y is horizontal direction and axis Z is through the origin of coordinates and vertically pointed to the paper face. In Fig. 3, assuming that the number of balls simultaneously loaded in each row of balls is n_s, the contact angles of the balls are α, and D_b is the diameter of the ball. The load of balls bearing in one row is $Q_i (i = 1, 2, 3, 4)$. Q_0 is the preload of each row.

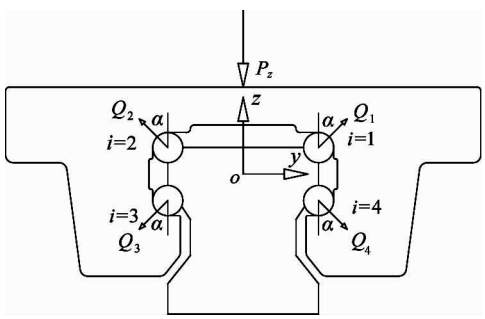

Fig. 3 Force analysis of ball linear rolling guide

According to Hertz contact theory[9], the contact area between ball and raceway is a slender ellipse. The elliptic parameters of contact area of steel ball guide are calculated as follows:

$$a = m_a[3Q_{ij}/(2E'(A + B))]^{1/3} \quad (23)$$

$$b = m_b[3Q_{ij}/(2E'(A + B))]^{1/3} \quad (24)$$

$$\cos\theta = \frac{B - A}{B + A} \tag{25}$$

$$A + B = \frac{1}{2}(\rho_{11}^{-1} + \rho_{12}^{-1} + \rho_{21}^{-1} + \rho_{22}^{-1})$$

$$B - A = \frac{1}{2}\left[(\rho_{11}^{-1} - \rho_{12}^{-1})^2 + (\rho_{21}^{-1} - \rho_{22}^{-1})^2 + 2(\rho_{11}^{-1} - \rho_{12}^{-1})(\rho_{21}^{-1} - \rho_{22}^{-1})\cos 2\gamma\right]^{1/2} \tag{26}$$

where, ρ_{11} and ρ_{12} are the curvatures of ball in two orthogonal directions, respectively, and ρ_{21} and ρ_{22} are the curvatures of raceway in two orthogonal directions. a and b are the ellipse contact short half axes and long half axes. m_a and m_b are the coefficients related to the elliptic principal curvature function. E' is synthetic curvature of ball. According to the sum of principal curvatures and the functions of principal curvature, m_a and m_b can be obtained. γ can be taken as 0° or 90°. Q_{ij} is the external load on any one ball.

Assuming K_a is the Hertz contact stiffness coefficient, contact deformation between the ball and raceway can be obtained:

$$K_a = \frac{3K}{\pi\mu}\left[\left(\frac{1 - \nu_1^2}{E_1} + \frac{1 - \nu_2^2}{E_2}\right)^2 \cdot \frac{\sum\rho}{3}\right]^{1/3} \tag{27}$$

where, $3K/\pi$ are the coefficients related to the elliptic principal curvature function. $\sum\rho$ is the summation function of the curvatures. v_1 and v_2 are the Poisson's ratio, E_1, E_2 are the elastic modulus of the ball and the raceway respectively. Then, the deformation of the ith column, jth ball is δ_{ij}, and the relationship between the external loads Q_{ij}:

$$\delta_{ij} = K_a \cdot Q_{ij}^{2/3} \tag{28}$$

$\sum\rho$ is the function of curvature, as shown in:

$$\sum\rho = \rho_{11} + \rho_{12} + \rho_{21} + \rho_{22} \tag{29}$$

Due to the preload, the relationship between deformation of balls in single row and the force is shown in Eq. (30).

$$\delta_0 = K_a \cdot Q_0^{2/3} \tag{30}$$

Therefore, the deformation of the ball in one row in the vertical direction is δ_z, shown in Eq. (31).

$$\delta_z = (\delta + \delta_0)\cos\alpha \tag{31}$$

2.2 Contact area analysis between ball and raceway

With the gradual increase of vertical load, the contact area also increases, speeds of ball and rail are different, and the tangential force of the bearing ball is also different, creep rate also changes when ball and rail contacts, the distribution of adhesion and micro-slip area is shown in Fig. 4. Under the ball bearing pressure and tangential force, the adhesive area in the contact area is S_s, λ_b is the ratio between the long half axes of the adhesive region and the long half axes. And λ_a is the ratio between the short half axes of the adhesive region and the short half axes. The contact area of adhesion is

$$S_\varepsilon = \pi a_\varepsilon b_\varepsilon = \lambda_a\lambda_b\pi ab \tag{32}$$

Combing Eqs (17) and (18), Eq. (33) is obtained:

$$\begin{aligned}\lambda_a - 1 &= D_b\zeta_x/(2a\mu)\\ \lambda_b - 1 &= D_b\zeta_y/(2b\mu)\end{aligned} \tag{33}$$

Substituting Eq. (33) into Eq. (32):

$$S_\varepsilon = \pi ab[(D_b\zeta_x/2a\mu) + 1][(D_b\zeta_y/2b\mu) + 1] \tag{34}$$

According to the adhesive area, the smoothing area S_s can be obtained:

$$S_s = \pi ab - \lambda_a\lambda_b\pi ab \tag{35}$$

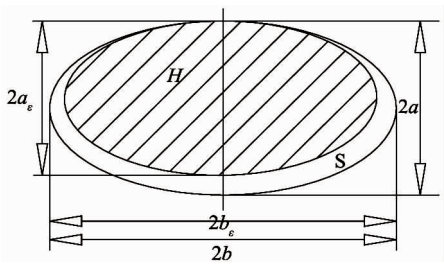

Fig. 4 Distribution of adhesive area

2.3 Analysis on friction coefficient

Conventionally, the ratio of the rolling friction torque to the normal load is defined as the rolling friction coefficient, In Fig. 5, e is the displacement due to the rolling resistance, δ_{ij} is the double-side indentation depth of the i-th row, and the j-th ball. The speed of the slider is in the positive direction of axis X, and the friction is f_b. N is the force of ball bearing.

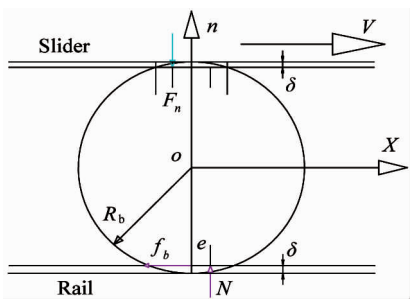

Fig. 5 Analysis on friction between ball and rail

According to the curve in Fig. 5, the force balance equation is established. $F_n \cdot e = f_b \cdot (R_b - \delta_{ij})$. So, the rolling friction coefficient is:

$$\mu_b = f_b/F_n = e/(R_b - \delta_{ij}/2) \tag{36}$$

For ball and raceway contact, e may be taken as $e = 3\tau \times 2a/16$, where, τ is the elastic lag coefficient, a is the half axes of the contact area in the rolling di-

rection, respectively. And $\tau = 3 \times 0.3$ for the case where the long axis of the contact area is much larger than the short axis. Rail friction coefficient μ_b is

$$\mu_b = e/(R_b - 0.5K_a Q^{2/3}) \tag{37}$$

3 Model of creep fractal wear

3.1 Raceway fractal surface and parameters

Assume that the microscopic roughness of ball-to-raceway contact plots obey the island distribution. The sticky regions in the creep state are divided into a series of 8 × 8 μm discrete differential surfaces. The differential surface can be characterized by W-M function[10].

$$z(x) = G^{D'-1} \sum_{n=n_l}^{\infty} \gamma^{(D'-2)n} \cos(2\pi\gamma^n x) \tag{38}$$

where, $z(x)$ is the random contour height of the rough surface, x is the coordinate position of the contour, G is the characteristic scale factor of the fractal surface, D' is the fractal dimension of the surface profile, γ^n determines the frequency spectrum of the rough surface, there $\gamma = 1.5$ is assumed. Fractal parameters can be obtained by structural function method, the contour structure function is defined as

$$E(\tau) = \langle z(x+\tau) - z(x) \rangle^2 \tag{39}$$

where, τ is any increment in the x direction and $E(\ )$ is the square of the mean of the plane.

3.2 Analysis of fractal contact mechanics

The contact of the ball with the raceway is considered as a rigid surface in contact with a surface having fractal characteristics. The truncated dimension of rigid rough surface to rough surface obeys island distribution, and the truncated size distribution of 3D asperity is[11]:

$$n(A) = (D-1)(A_L/A)^{(D+1)/2}/2A_L \tag{40}$$

where, A is the contact area of the asperity on the contact surface, A_L is the maximal cut-off contact area of the asperity, D is the surface fractal dimension, and the relation between D and D' in Eq. (38) is $D = D' + 1$. According to differential-shaped surface elasto-plastic analysis the following can be obtained[11]:

$$A_c = [2^{11-2D} G^{2D-4} E^* \ln\gamma/(9\pi^{4-D} H)]^{1/(D-2)} \tag{41}$$

$$F_e = \frac{2^{\frac{(11-2D)}{2}}}{3\pi^{(4-D)/2}} \left(\frac{D-1}{5-2D}\right) (\ln\gamma)^{1/2} G^{D-2} E^* (A_L)^{(4-D)/2} [1 - (A_c/A_L)^{(5-2D)/2}] \tag{42}$$

$$F_p = ((D-1)Ha_L/(3-D))(A_c/A_L)^{(3-D)/2} \tag{43}$$

$$S = [(D-1)/(6-2D)][1 + (A_c/A_L)^{(3-D)/2}] a_L \tag{44}$$

where, E^* is the integrated elastic modulus, H is the hardness of the slider material, and the yield strength σ_s of the material, generally take $H = 2.8\sigma_s$. F_e is the sum of the differential surface elastic load, and F_q is the sum of the plastic load of the micro fractal surface, A_c is the critical truncated contact area of the asperity. When $A \leqslant A_c$, the asperity deforms into plastic deformation. Body deformation is elastic deformation. S is the total contact area between the micro-shaped surface and the rigid plane.

Total load F_z of the differential surface is the sum of the elastic load and the plastic load:

$$F_z = F_e + F_p \tag{45}$$

In order to reduce wear and extend the service life of linear guide, thin oil lubrication is used between the ball and the rail. Assuming that the lubrication between the ball and the raceway is a boundary lubrication state, it is proved that the hydrodynamic pressure generated between two of asperities surface is approximately equal to the yield strength σ_s of the softer material in the friction pair[12]. Assuming that all differential surfaces uniformly bear the pressure of the adhesive contact surface, the analysis of the micro-fractal surface forces can be obtained:

$$\sigma_s(A_\alpha - S) + F_z = P_{mz} A_\alpha \tag{46}$$

where, the differential surface nominal area $A_\alpha = 64\mu m^2$, P_{mz} is for contact elliptical adhesive zone average contact stress. The maximal cut-off contact area A_L is obtained by

$$K_1 A_L + K_2 A_L^{(4-D)/2} + K_3 A_L^{(D-1)/2} - K = 0 \tag{47}$$

where, K, K_1, K_2, K_3 are given in Ref. [13].

3.3 Fractal wear volume model

According to the W-M fractal function, it can be seen that the contour line of the asperity above the bottom circle can be approximated as cosine wave, and the function expression is[14]:

$$z(x) = G^{D-2} l^{3-D} \cos(\pi x/l) \quad -l/2 < x < l/2 \tag{48}$$

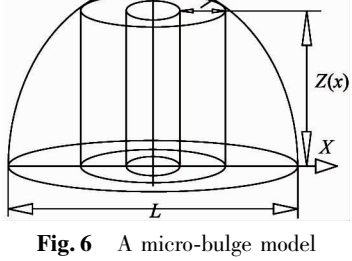

Fig. 6 A micro-bulge model

According to the curve relation in Fig. 6, the volume of one asperity V (A) can be obtained by[15]

$$V(A) = (\pi - 2) 2^{4-D} G^{D-2} A^{(5-D)/2} / \pi^{(7-D)/2} \tag{49}$$

Assuming that the asperity is approximately an axisymmetric body and the base circle diameter of the contact surface is l, the relationship between the sectional contact area S_0 and the base circle radius l of a single asperity is

$$l^2 = 4S_0/\pi \tag{50}$$

When the relative sliding occurs between a single ball and raceway, the relative distance l_a can be got:

$$l_a = \frac{\int_0^4 n(A) l \mathrm{d}A}{\int_0^4 n(A) \mathrm{d}A} = \frac{2(D-1)}{\sqrt{\pi}(D-2)} A_c^{1/2} \tag{51}$$

Due to the presence of creep between the ball and rail, it is assumed that wear of the balls and raceways occurs in the micro-slide area rather than the entire Hertz contact zone. The total volume of debris ΔV[15] due to the relative sliding of the ball and the raceway is

$$\Delta V = \frac{S_s(\pi-2)2^{3-D}G^{D-2}A_L^{(D-1)/2}A_c^{3-D}(D-1)}{A_\alpha(3-D)\pi^{(7-D)/2}} \tag{52}$$

Therefore, the wear volume V_0 per unit length between the single ball and the raceway is

$$V_0 = \Delta V / l_a \tag{53}$$

According to Section 1.2, creep rate analysis shows that the ball in the raceway runs L_x mileage at a certain speed, the ball in the slider track on the actual relative sliding distance l_s can be calculated by

$$l_s = \zeta_x L_x \tag{54}$$

As the wear is in process, not all of the micro-slip area of adhesive points will produce debris, so the introduction of fractal wear coefficient is K_f, the wear volume should be corrected. Then, V_i is the wear volume of the ith row ball after running L_x mileage.

$$V_i = n_s K_f V_0 l_s \tag{55}$$

Comprehensively, from Eqs(51) – (55), Eq. (56) can be obtained

$$V_i = K_f n_s A_L^{(D-1)/2} S_0 \frac{(ab - a_\varepsilon b_\varepsilon)\zeta \pi^{(D/2-2)}(\pi-2)(D-2)}{2^{D-3}A_\alpha(3-D)G^{2-D}A_c^{(D-5/2)}} \tag{56}$$

The total wear of each row of balls is uniformly distributed in the rectangular region with length l_r and width $2b$ of the slider with the movement of the balls. Therefore, the normal wear depth h of the corresponding raceway contact surface caused by the ith row ball is

$$h_i = V_i/(2l_r b) \tag{57}$$

$$l_r = D_w(n_s - 1)D_b + D_b \tag{58}$$

where, D_w is the ratio of the distance between two adjacent balls to the ball diameter. From Eqs(56) – (58), Eq. (59) is obtained:

$$h_i = \frac{K_f n_s (ab - a_\varepsilon b_\varepsilon)\zeta \pi^{(D/2-2)}(\pi-2)(D-2)A_L^{(D-1)/2}S_0}{2^{D-2}b(D_w(n_s-1)+1)D_b A_\alpha(3-D)G^{2-D}A_c^{(D-5/2)}} \tag{59}$$

As the wear between the ball and the roller raceway occurs, therefore, the wear amount δ_{bs} of the slider is half of the total wear depth.

$$\delta_{bs} = 0.5h_i \tag{60}$$

In Fig. 3, after a period of time, the rolling linear guideway is subjected to load, the deformation of wear $\Delta\delta_{bs}$ between the slider track and the ball in the vertical direction is

$$\Delta\delta_{bs} = \delta_{bs}\cos\alpha \tag{61}$$

Therefore, the total displacement amount δ_c of the linear guide in the vertical direction after wear is the sum of the contact deformation amount δ_z and the vertical wear amount $\Delta\delta_{bs}$. According to Eq. (29), Eq. (62) can be obtained:

$$\delta_c = \delta_z + \Delta\delta_{bs} \tag{62}$$

When the ball linear guide wears, the ball preload force is degraded and the initial deformation amount is small. In the calculation of the wear amount, the initial deformation amount needs to be amended to ensure the calculation accuracy with the increase of the running mileage. The variation $\delta_{(i+1)0}$ of the initial preload and deformation δ_0 of each row of balls with the wear process can be obtained:

$$\delta_{(i+1)0} = \delta_{i0} - 0.5h_i \tag{63}$$

4 Simulation and analysis

4.1 Calculation of related parameters of rolling guide

The LG20-type guide is selected as the research object. The main parameters are shown in Table 1.

Table 1 the main parameters of the LG20-type guide

Initial deformation δ_0(mm)	0.004
Diameter of ball D_a(mm)	3.969
Curvature ratio f	0.51
Bearing ball number n_s	12
Contact angle α(°)	45

Slider and ball materials are high-carbon chromium bearing steel GCr15, $E^* = 1.143 \times 105$ MPa, $\sigma_s = 518.4$ MPa. Su et al.[16] showed that the wear coefficient decreased with the load and tended to a stable value, taking $K_f = 5 \times 10^{-4}$. The wear and loss of ball linear guide pair were simulated by the law of degradation.

4.2 Calculation on long and short half-shaft of Hertz contact ellipse

The contact parameters of LG20 ball are simulated by Matlab. The relationship between the ellipsoidal long (short) axis of the contact area and the external load is shown in Fig. 7.

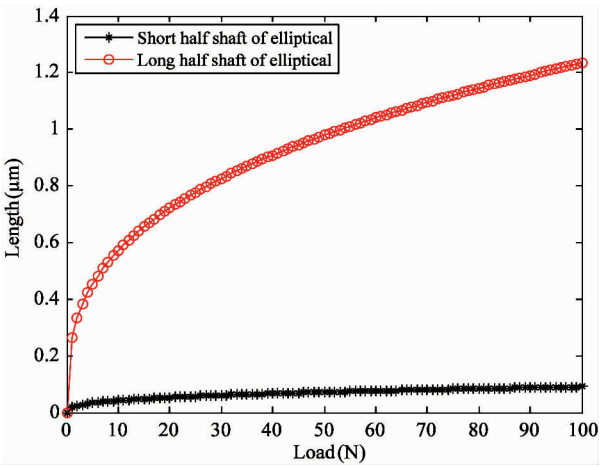

Fig. 7 Relationship between the long and short half axes of the Hertz contact elliptical and external load

The relationship between the contact area of the ellipse and the load is shown in Fig. 8.

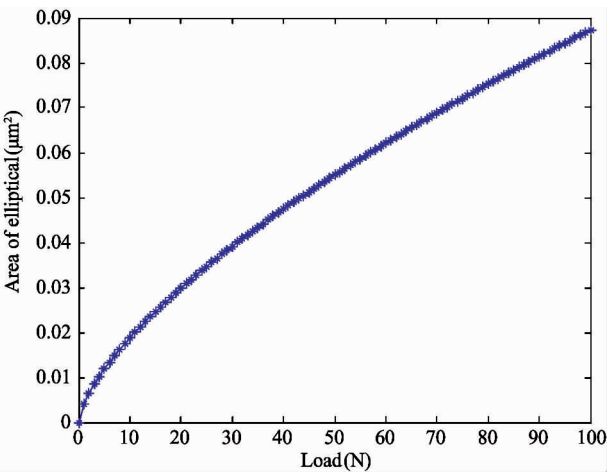

Fig. 8 Area of Hertz contact elliptic and external load

As shown in Fig. 7 and Fig. 8, it can be seen that the contact zone is a narrow oval. The contact area between ball and raceway increases nonlinearly with the increase of load.

4.3 Relationship between the creep-slipping area and the Hertz ellipse area

The relationship between the length of the long axes of the adhesive zone (α_ε) and the tangential force (F_L) is shown in Fig. 9.

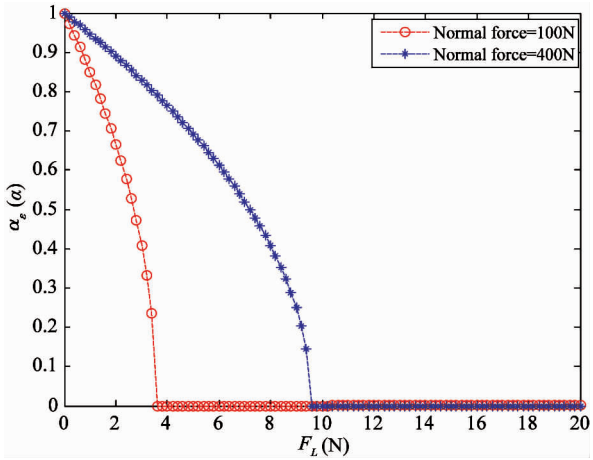

Fig. 9 Ratio of the long axes of the adhesion area to that of Hertz area

When the ball bears the normal force only the tangential force is zero, while the ball begins to move, tangential force begins to work, tangential adhesion area becomes small, tangential force gradually increases until the adhesive area disappears, complete sliding between the ball and the raceway occurs.

4.4 Calculation on the area of adhesion area under creeping condition

When the external load is equal to a constant, the size of the contact area will not change. And the area of the adhesive zone will change with the running speed of slider. In Fig. 10, when the external load is 1kN, the relationships between the tangential force and the area of the adhesive zone are simulated under considering lateral creep and neglecting lateral creep.

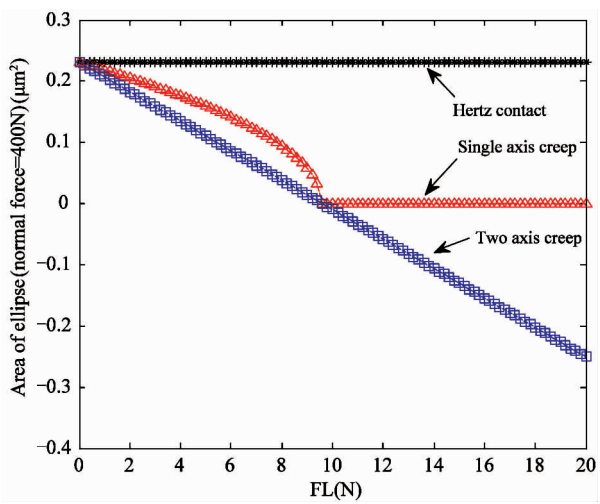

Fig. 10 Relationship between tangential force and the area of the adhesive area

The area of the creep zone increases with the increase of the tangential force, when the external load is equal to 1kN. As shown in Fig. 10, the horizontal line is the Hertz contact elliptical area, which does not vary with the change of the tangential force. After considering the lateral creep rate, the change trend of adhesive wear area is not the same.

4.5 Calculation on friction coefficient and friction

According to the model, rolling friction coefficient as a function of external load (see Fig. 11) increases with the corresponding increase in external load. The friction coefficient increased remarkably when the external load was increased to 160 N. In this paper, the stress of single ball is calculated separately when the external load is 150 N and 2 kN, so the friction coefficient $\mu < 0.03$.

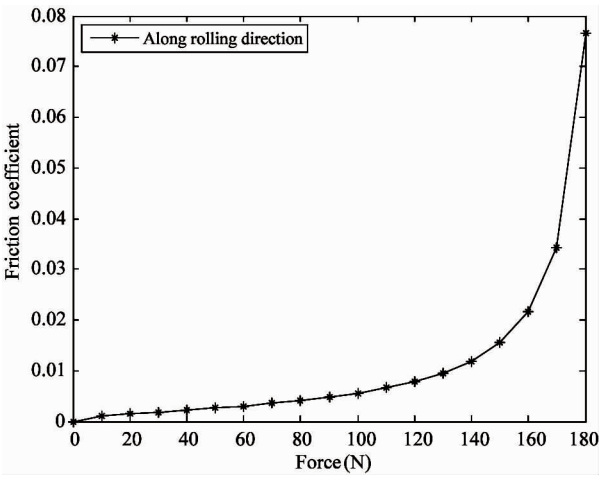

Fig. 11 Relationship between friction coefficient and load

4.6 Analysis on fractal parameter base on experimental data

The surface profile of LG20 is measured by the microscope system. The measurement area is 500 μm ×675 μm, and the number of sampling points is 768 ×1 024. Fractal parameters D' and G can be obtained by the power spectral function method. In 675 μm length choose 675 data points, $G = 2.38 \times 10^{-8}$ m, using the least square method to fit the double logarithm of the structure function. Fig. 12 shows a section of the measured profile of the raceway surface. Fig. 13 is a log-log plot of the structural function using the least-squares fitting plot.

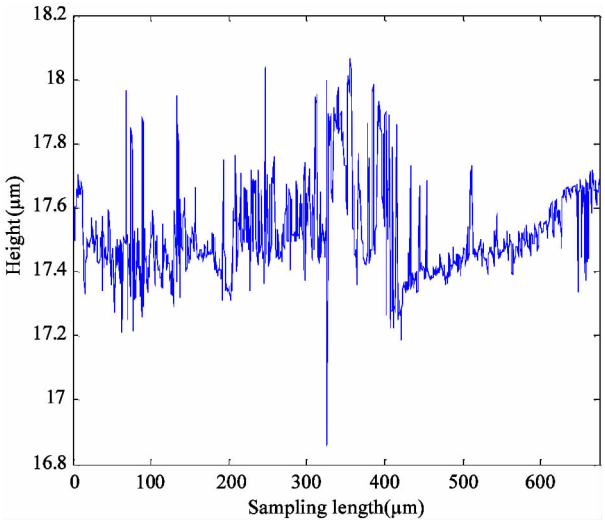

Fig. 12 Curve of surface profile height on the raceway

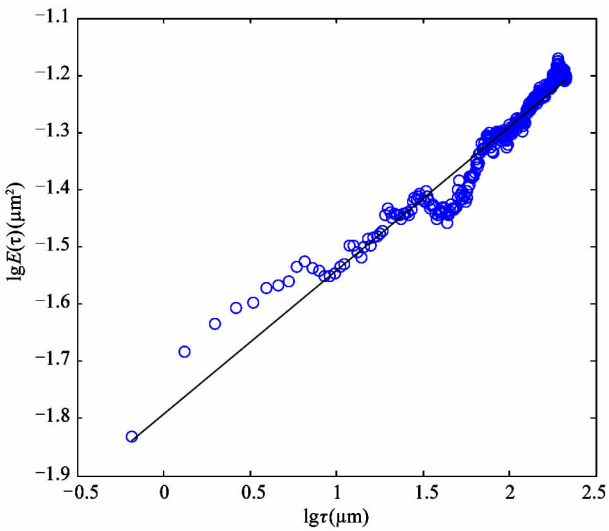

Fig. 13 Double logarithmic graph of structure function

4.7 Wear calculation of linear rolling guide

Fig. 14 shows the simulation results when the rolling linear guide runs at 5 km. It can be seen from the curve that the bigger the load is, the larger the total deformation is, and the elastic deformation and the displacement of the slide are. The simulation curve of the elastic deformation δz is consistent with the vertical stiffness curve of the ball linear guide pair. From Fig. 14 it can be seen that when the external load is large, the slider elastic deformation δz is much greater than the amount of wear generated by wear, the total slider displacement curve and elastic deformation curve of the trend is changed.

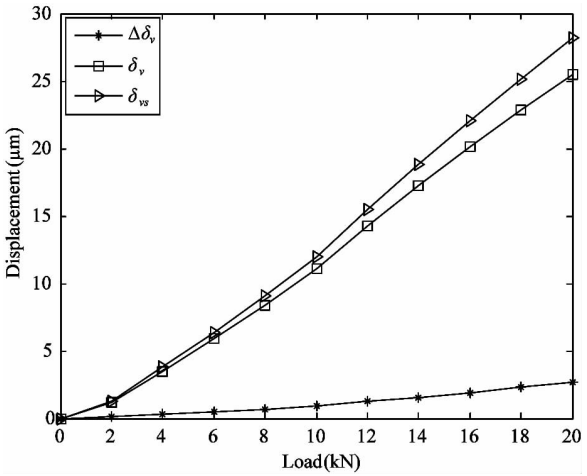

Fig. 14 Displacement when the running distance is 5 km

Fig. 15 and Fig. 16 show three cases of creep rate of sliding total wear $\Delta\delta_{bs}$ and the total displacement of δ_c curve. Obviously, the greater the creep rate is, the smaller adhesion area is. As mileage increases, the rate of growth of total wear in the vertical direction slows down.

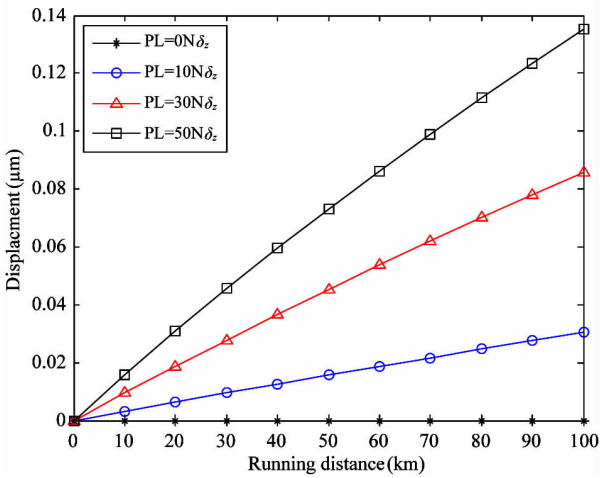

Fig. 15 Displacement of slider due to wear under force is 2 kN

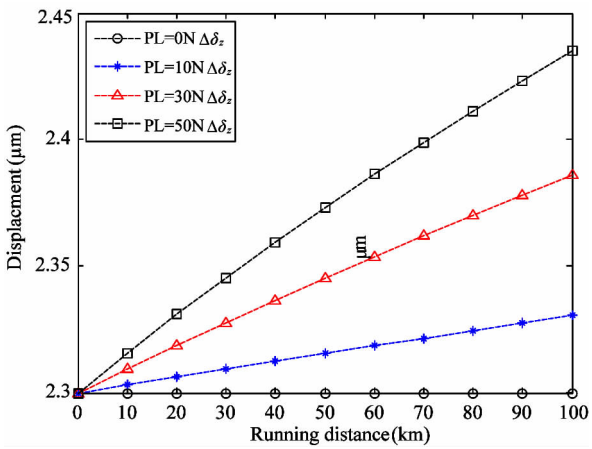

Fig. 16 Total displacement of the slider under force being 2 kN

Under constant external loads, the elastic deformation of LG20 linear guide δ_v is approximately constant, In Fig. 17, the difference between the upper and lower curves is the amount of elastic deformation of the ball. The curve shows that the difference between the two sets of curves is almost unchanged. The total displacement in the vertical direction increases with the running distance, and the proportion of the displacement caused by the wear is increasing, leading to the decrease of the guide accuracy of the linear rolling guide. When the amount of displacement in the normal direction caused by the wear of the raceway exceeds the preloading initial deformation of the ball, the contact between the balls and the raceway in the next two rows of the slider results in loss of rigidity.

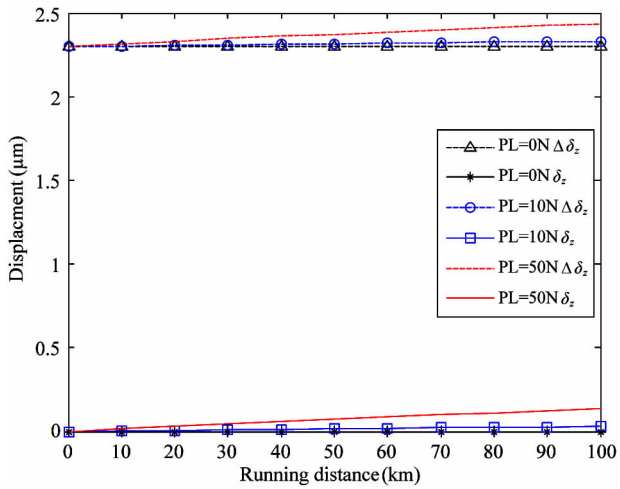

Fig. 17 Total displacement of the slider under force being 2kN

5 Conclusions

The model of creep-fractal friction takes into account the adhesive contact area, micro slip area, fractal parameters of the contact surface and the dynamic pressure of the lubricating medium. This model can more realistically reflect the real friction condition of the raceway. The wear is closely related to the motion state of the ball and the parameters of the creep state.

The influence of creep rate and load on contact area is considered. The size of the micro slide zone is calculated as the motion velocity changes. After considering creep, the friction loss of the raceway is smaller than that without creep.

Combined with creep and fractal theory, the parameters of rail are analyzed, and the influence of load on friction coefficient is analyzed. The results show that the creep is related to the operation of rail. The change of bidirectional creep rate is different from that of unidirectional creep. This magnitude has a greater

influence on the adhesive area. The greater the speed is, the greater the micro slip area is, so the greater friction loss of the raceway is.

The proposed model can provide a theoretical basis for the study of the accuracy degradation law and the accuracy retention test of the linear guide pair. Considering the creep phenomenon, the wear degree of raceway is lower than that of traditional thin oil lubrication.

Reference

[1] Zhong Y. Study on the Theoretical Research of Accuracy Preservation of the Linear Ball Guide and Experimental Design [D]. Nanjing: Nanjing University of Science and Technology, 2014. 35-68 (In Chinese)

[2] Ge S R, Zhu H, Li D. The Fractal of Tribology [M]. Beijing: Mechanical Industry Press, 2005. 112-124 (In Chinese)

[3] Zhou G Y, Leu M C, Blackmore D. Fractal geometry model for wear prediction [J]. *Wear*, 1993, 170(1): 1-14

[4] Chen G A, Ge S R, Wang J X. Application of fractal geometry in tribology [J]. *Tribology*, 1998, 18(2): 179-184

[5] Fang G F, Teng W R, Liu Q, et al. Adhesive wear fractal model for end face of mechanical sals [J]. *Fluid Machinery*, 2013, 41(1): 35-41 (In Chinese)

[6] Kalker J J. Three-Dimensional Elastic Bodies in Rolling Contact [M]. Xi'an: Xi'an Jiao Tong University Press, 1993. 99-135

[7] Kong X A, Jiang X Y, Jin X S. Solid Contact Mechanics [M]. Beijing: China Railway Publishing House, 1999. 34-55 (In Chinese)

[8] Johnson K L. The effect of a tangential contact force upon the rolling motion of an elastic sphere [J]. *Journal of Applied Mechanics*, 1958, 25: 339-346

[9] Wen S Z, Yang P R. Elastic-hydrodynamic Lubrication [M]. Beijing: Tsinghua University Press, 1992. 88-102 (In Chinese)

[10] Majumdar A, Tien C L. Fractal characterization and simulation of rough surfaces [J]. *Wear*, 1990, 136(2): 313-327

[11] Yan W, Komvopoulos K. Contact analysis of elastic-plastic fractal surfaces [J]. *Journal of Applied Physics*, 1998, 84(7): 3617-3624

[12] Li C Q. Machine Tool's Friction and Wear and Lubrication [M]. Beijing: China Machine Press, 1990. 97-100

[13] Wang M, Jiang X F, Zhang W. Fractal wear model and accuracy degradation of linear ball guideways [J]. *Chinese High Technology Letters*, 2016, 26(3): 275-282 (In Chinese)

[14] Majumdar A, Bhushan B. Fractal model of elastic-plastic contact between rough surfaces [J]. *Journal of Tribology*, 1991, 113(1): 1-11

[15] Wang X H, Zhang S W, Fan Q Y. The model of the adhesive wear based on the theory of fractal geometry [J]. *Journal of the University of Petroleum*, 1999, 23(6): 50-53 (In Chinese)

[16] SU Y W, Chen W, Zhu A B, et al. Contact and wear simulation between fractal surfaces [J]. *Journal of Xi'an Jiao Tong University*, 2013, 47(7): 52-56 (In Chinese)

Zhang Wei, born in 1979. He received his M. S. degree in Mechanical and Electronic Engineering Department of Inner Mongolia University of Science and Technology in 2009. He also received his B. S. degree from Inner Mongolia University in 2003. His research interests include the rapid prototyping technology and accuracy of CNC machine tools.